Journal of Molecular Structure 982 (2010) 91–99

Contents lists available at ScienceDirect

Journal of Molecular Structure

journal homepage: www.elsevier.com/locate/molstruc

# Effect of fluorine substitution on the crystal structures and vibrational properties of phenylthiourea isomers

Aamer Saeed [a,*], Mauricio F. Erben [b], Ulrich Flörke [c]

[a] Department of Chemistry, Quaid-I-Azam University, Islamabad 45320, Pakistan
[b] CEQUINOR (UNLP, CONICET-CCT La Plata), Departamento de Química, Facultad de Ciencias Exactas, Universidad Nacional de La Plata, C.C. 962 (1900), La Plata, Argentina
[c] Department Chemie, Fakultät fur Naturwissenschaften, Universitat Paderborn, Warburgerstrasse 100, D-33098 Paderborn, Germany

ARTICLE INFO

*Article history:*
Received 8 June 2010
Received in revised form 5 August 2010
Accepted 5 August 2010
Available online 11 August 2010

*Keywords:*
1-(2-Chlorobenzoyl)-3-(isomeric fluorophenyl)thioureas
Crystal structure
Conformer
Hydrogen bonds
Quantum chemical calculations
Vibrational studies

ABSTRACT

The 1-(2-chlorobenzoyl)-3-(isomeric fluorophenyl)thiourea derivatives (**1**–**3**) were prepared by the reaction of 2-chlorobenzoyl isothiocyanate produced *in situ* with isomeric fluoroanilines in excellent yields. The novel compounds are characterized by multinuclear ($^{1}$H and $^{13}$C) NMR, GC–MS, elemental analyses and FTIR spectroscopy techniques. Structural and conformational properties of compounds **1**–**3** are analyzed using a combined approach including X-ray diffraction, vibrational spectra (solid FTIR and FT-Raman) and theoretical calculation methods. The crystal structures have been determined by X-ray diffraction methods. The three species crystallize in the monoclinic C2/c space group with and $Z = 8$ molecules per unit cell. The carbonyl and thiourea groups are almost planar and the conformation adopted by the C=S and the C=O double bonds is antiperiplanar. The crystal lattices show the presence of centrosymmetric dimeric units held by N–H···S hydrogen bonds stacked along the [0 1 0] plane. The effect of fluorine substitution on the vibrational properties and on the conformational space has been determined by quantum chemical calculations (B3LYP functional in connection with the 6-311+G* basis sets) and vibrational spectroscopy.



## 1. Introduction

1-Aroyl-3-arylthioureas containing both carbonyl and thiocarbonyl groups can coordinate to metals using both sulphur and oxygen atoms, the presence of these hard and soft donor sites offer a huge bonding potential [1,2]. Thus, besides the academic interest, *N*,*N*-dialkyl-*N*-aroyl thioureas are efficient ligands for the separation of platinum group metals [3]. Thiourea complexes are starting materials in chemical spray pyrolysis (CSP) processes which are used to produce thin films of binary and ternary sulfides [4].

Moreover, fluorinated aryl thioureas represent a new class of potent anti-trypanosomal agents [5] and also a novel class of potent influenza virus neuraminidase inhibitors [6]. 1,3-Dialkyl or diaryl thioureas exhibit significant antifungal activity against plant pathogens *Pyricularia oryzae* and *Drechslera oryzae* [7].

*N*-aryl *N*-phenyl thioureas have been developed as anion-binding site in a hydrogen-bonding receptor [8]. Thiacalix[4]arenes containing thioureas are neutral receptors towards α,α-dicarboxylate anions [9] and *N*-4-substituted-benzyl-*N*′-*ter*-butylbenzyl thioureas are vanilloid receptors ligands and antagonists in rat DRG neurons [10]. 1-Benzoyl-3-(4,6-disubstituted-pyrimidinyl) thioureas have shown excellent herbicidal activity [11]. Thioureas have also extensively been used in enantioselective synthesis, such as nitro-Mannich reactions, Aza-Henry reaction and the Michael Addition [12–14]. Fabbrizzi et al. reported that substituted-phenyl urea compounds interacts through hydrogen bonding with a variety of oxoanions to give bright colored complexes [15]. A variety of receptors containing the urea and the thiourea groups have been designed for anion recognition [16]. In this context, the molecular structure and conformational flexibility are important properties for determining the donor–acceptor capabilities [17]. Also the thioureas can denature proteins, and inhibit the formation of micelles. Therefore the conformational issues in thioureas are comparable to those arising in folded proteins, and a complete understanding of these effects require understanding the effects of intermolecular hydrogen bonding interactions and hydrophobic interactions [16].

Recently, fluorinated thioureas have been reported as convenient synthons for preparation of versatile fluorine-containing heterocycles [18]. Taking into consideration the aforementioned biological, synthetic and theoretical importance of thioureas, here we report the synthesis and structural characterization of three novel 1-(2-chlorobenzoyl)-3-(isomeric fluorophenyl)thiourea derivatives (**1**–**3**). The vibrational properties have been studied by infrared and Raman spectroscopy along with quantum chemical calculations.

* Corresponding author. Tel.: +92 51 9064 2128; fax: +92 51 9064 2241.
*E-mail address:* aamersaeed@yahoo.com (A. Saeed).

0022-2860/$ - see front matter © 2010 Elsevier B.V. All rights reserved.
doi:10.1016/j.molstruc.2010.08.012

## 2. Results and discussion

### 2.1. X-ray structure

ORTEP [19] drawing of the molecular structures of compounds **1**–**3** as determined in the crystalline phase are shown in Figs. 1–3, respectively and Table 1 includes selected geometric parameters derived from the structure refinement, as well as those obtained from quantum chemical calculations.

The three molecular structures differ from the fluoro-substitution pattern of the benzamide ring. Minor differences have been observed in the molecular geometry determined for the three isomers when the crystal structure is compared. For example, the two aromatic planes form dihedral angles each of 26.94(6)°, 23.93(8)° and 42.64(5)° for **1**–**3**, respectively. The carbonyl and thiourea groups O1/C1/N1/C8/S1/N2 are almost planar, largest deviations from mean planes are 0.148(1), 0.121(1) and 0.092(1) Å for **1**, **2** and **3**, respectively. Associated are intramolecular N2–H···O1=C1 hydrogen bonds forming six-membered rings for all three structures. Dihedral angles between these carbonyl thiourea planes and the chlorophenyl/fluorophenyl rings measure for **1**: 69.59(3)°/43.34(4)°, for **2**: 71.94(5)°/48.11(5)° and for **3**: 74.83(4)°/39.91(4)°. The different fluoro substitution has no significant effect on N2–C9 or N2–C8 bond length parameters.

Crystal packing shows for **1**–**3** intermolecular N1–H···S=C hydrogen bonds, forming centro-symmetric dimers that are stacked along the [0 1 0] plane, as shown in Figs. 4–6, respectively. Intermolecular N1···S short distances amount 3.364(1), 3.379(1) and 3.348(1) Å for compound **1**–**3**, respectively. The shortest intermolecular C–H···F distances are in the 2.53–2.63 Å range, a short intramolecular N2–H···F distance in **1** measures 2.53 Å. The Cl atoms are not involved in hydrogen bonding.

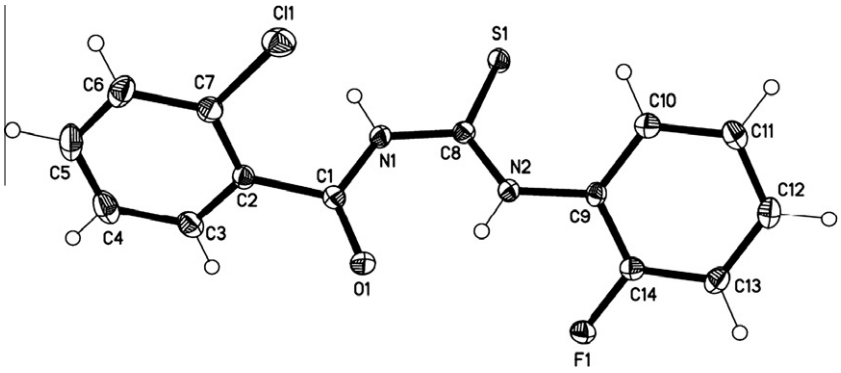


**Fig. 1.** Molecular structure of **1**. Displacement ellipsoids are shown at the 50% probability level.

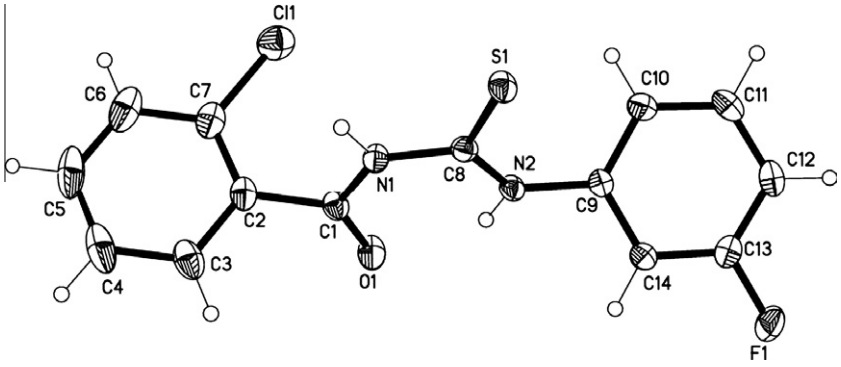


**Fig. 2.** Molecular structure of **2**. Displacement ellipsoids are shown at the 50% probability level.

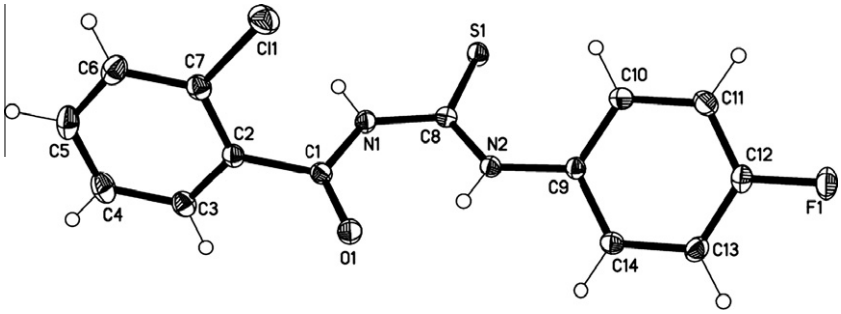


**Fig. 3.** Molecular structure of **3**. Displacement ellipsoids are shown at the 50% probability level.

**Table 1**
Experimental and calculated (B3LYP/6-311+G*) selected geometric parameters for the most stable conformer of compounds **1**–**3**.

| | 1 | | 2 | | 3 | |
|---|---|---|---|---|---|---|
| | Experimental | Calculated | Experimental | Calculated | Experimental | Calculated |
| *Bond lenghts* | | | | | | |
| C12–F1 | 1.3564(13) | 1.359 | 1.3571(19) | 1.355 | 1.3553(16) | 1.356 |
| N2–C9 | 1.3894(14) | 1.408 | 1.4250(19) | 1.411 | 1.4237(16) | 1.413 |
| C8–N2 | 1.3366(15) | 1.351 | 1.334(2) | 1.350 | 1.3333(16) | 1.347 |
| C8=S1 | 1.6729(11) | 1.670 | 1.6729(15) | 1.668 | 1.6730(13) | 1.670 |
| N1–C8 | 1.4181(14) | 1.412 | 1.3896(19) | 1.415 | 1.3920(16) | 1.416 |
| C1–N1 | 1.3753(14) | 1.377 | 1.3700(19) | 1.375 | 1.3706(16) | 1.374 |
| C1=O1 | 1.2200(13) | 1.225 | 1.2181(19) | 1.227 | 1.2231(16) | 1.228 |
| C1–C2 | 1.5012(15) | 1.504 | 1.504(2) | 1.504 | 1.5003(18) | 1.504 |
| C7–Cl1 | 1.7368(13) | 1.762 | 1.735(2) | 1.762 | 1.7371(14) | 1.761 |
| *Bond angles* | | | | | | |
| F1–C12–C11 | 118.10(10) | 117.7 | 117.69(15) | 118.3 | 118.48(12) | 119.0 |
| F1–C12–C13 | 119.09(10) | 119.0 | 119.02(15) | 119.0 | 118.73(12) | 119.3 |
| C8–N2–C9 | 125.63(9) | 131.1 | 125.43(13) | 132.3 | 127.01(10) | 132.3 |
| N2–C8=S1 | 125.98(9) | 129.4 | 125.80(12) | 129.7 | 126.49(10) | 129.7 |
| N1–C8=S1 | 118.26(8) | 116.4 | 118.18(11) | 116.5 | 117.68(9) | 116.4 |
| C8–N1–C1 | 128.28(10) | 130.2 | 128.57(13) | 130.3 | 128.71(11) | 130.2 |
| N1–C1=O1 | 122.54(10) | 123.0 | 123.62(14) | 123.1 | 123.94(12) | 123.1 |
| C2–C1=O1 | 123.81(10) | 120.3 | 122.64(14) | 120.1 | 122.52(11) | 120.1 |
| Cl1–C7–C2 | 120.16(9) | 122.1 | 119.05(15) | 122.1 | 119.41(11) | 122.1 |
| Cl1–C7–C6 | 118.64(10) | 116.8 | 119.74(15) | 116.8 | 119.20(10) | 116.8 |
| *Dihedral angles* | | | | | | |
| C9N2–C8=S1 | 6.3(4) | 0.9 | −4.8(4) | 0.5 | 7.3(5) | 0.6 |
| C1N1–C8N2 | −6.1(5) | 1.2 | 4.7(5) | 1.2 | −2.8(4) | 1.3 |
| C7C2–C1=O1 | 116.3(4) | 140.1 | 113.0(5) | 139.6 | 108.5(5) | 139.6 |
| C10C9–N2C8 | 45.8(4) | 7.6 | 50.3(5) | 0.6 | 40.0(5) | 0.0 |

### 2.2. Quantum chemical calculations

Prompted by the similar conformations found for the isomers (**1**–**3**) in the crystalline state, it was decided to examine the molecular structure of the studied compounds by using quantum chemical calculations at the DFT-B3LYP level of approximation. The comparison between experimental X-ray results with the corresponding computed structure for the molecule isolated in a vacuum could serves to better understand the conformational transferability observed for these substituted thioureas.

In principle the studied compounds may adopts several conformations mainly depending on the orientation around the thiourea moiety, the relative position of the C=O double bond and the orientation of substituted phenyl rings. Thus, to inspect the potential energy surface, in a first approximation the potential energy function for internal rotation around five central dihedral angles, i.e. around the N1–C8 and N2–C8 (for the thiourea group), the N1–C1 (for the relative orientation of the carbonyl bond) and N2–C9 and C2–C1 (F- and 2Cl-substituted phenyl rings) single bonds was calculated. The B3LYP method with the moderate 6-31G basis sets has been applied allowing geometry optimizations with the corresponding dihedral angle varying from 0° to 180° in steps of 20°. The potential energy curves are shown in Fig. 7 (for atom numbering see Figs. 1–3).

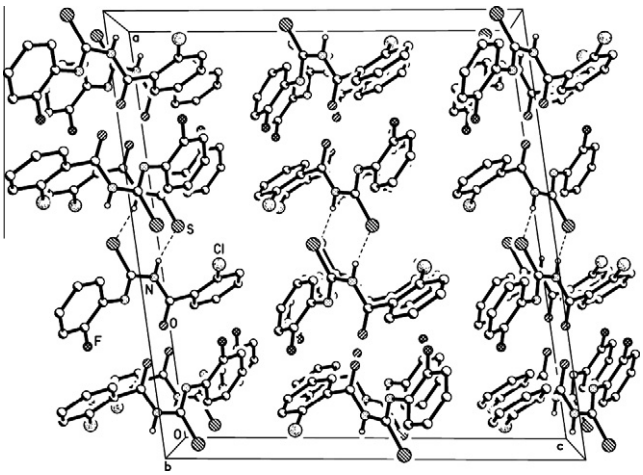


**Fig. 4.** Crystal packing of **1** viewed along [0 1 0] with intermolecular hydrogen bonding pattern indicated as dashed lines. H-atoms not involved in hydrogen bonding are omitted.

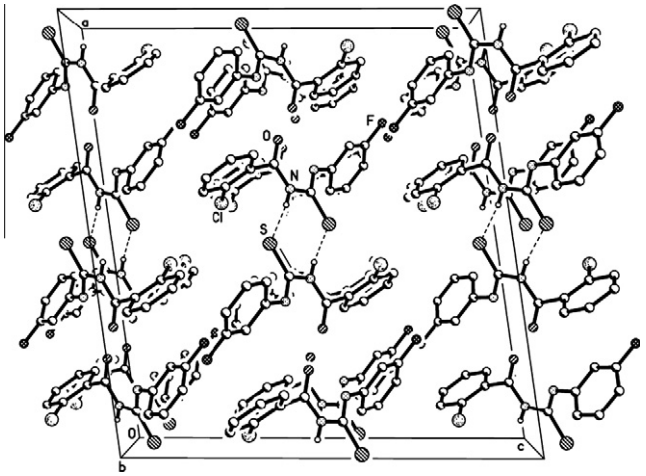


**Fig. 5.** Crystal packing of **2** viewed along [0 1 0] with intermolecular hydrogen bonding pattern indicated as dashed lines. H-atoms not involved in hydrogen bonding are omitted.

Very similar potential energy curves are obtained for the three compounds, except for the rotation of the fluorinated phenyl group (Fig. 7B). The curve obtained as a function of the dihedral angle around the C2−C1 bond, which is related to the formal rotation of the 2Cl-phenyl group, shows a deep minimum at $\delta$(C7C2−C1N1) ≈ 20°, corresponding to a structure with the C=O

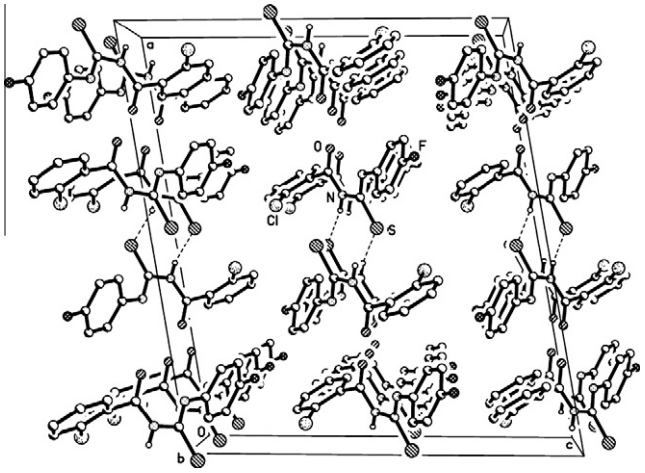

**Fig. 6.** Crystal packing of **3** viewed along [0 1 0] with intermolecular hydrogen bonding pattern indicated as dashed lines. H-atoms not involved in hydrogen bonding are omitted.

and C–Cl bonds in mutual synclinal orientation (Fig. 7A). The maxima observed at $\delta$(C7C2−C1N1) = 180° correspond to planar structures with the C–Cl and the C=O bond in a mutual eclipsed position for the three species.

The curves obtained by rotation of the F-phenyl group show minima at $\delta$(C8N2–C9C10) = 0° for the three studied isomers, corresponding to molecular structures having the F-$C_6H_4$-ring and the thiourea group in a planar arrangement. As expected, the curve obtained for the 4-F species shows equivalent minima at dihedral angle values of 0° and 180°, whereas the second conformation is slightly preferred for isomer **3**. In contrast, a pronounced maxima is observed for **2** at $\delta$(C8N2–C9C10) = 180°, when the C–F and C=S bond are eclipsed, denoting strong repulsive interactions between the fluorine atom and the C=S double bond. These curves are shown in Fig. 7B.

The potential energy curves for the rotation around the N1–C(S) bond in the thiourea moiety are very similar for the three studied species, with minima at $\delta$(C1N1−C8S1) dihedral angle values of ca. 30° and 180° corresponding to synclinal and anti forms, respectively, with a local planar arrangement for this moiety. As can be observed in Fig. 7C, the anti conformation of the C=S bond with respect to the N1−C1 bond is more stable by ca. 14.5 (**1**) and 15.5 (**2**, **3**) kcal mol$^{-1}$ than the synclinal conformer [$\delta$(C1N1–C8S1) ≈ 30°]. When the second dihedral angle involving the thiourea group is studied, i.e. $\delta$(C9N2–C8S1), the potential energy curves show the presence of two minima at $\delta$(C9N2–C8S1) = 0° and a second minimum at ca. 160°, as observed in Fig. 7D. The last one, higher in energy by ca. 10 kcal mol$^{-1}$, corresponds to a structure with both C–N bonds antiperiplanar with respect to the C=S double bond.

Finally, the potential energy curve obtained for variation of the $\delta$(C8N1–C1O1), showed in Fig. 7E is similar to those expected for a typical amide moiety, showing two minima for conformers having syn and antiperiplanar orientation of the C=O and N–C(S) bonds, the former being much more stable than the second one.

Additionally, full geometry optimizations and frequency calculations were computed for each of the minima previously found for the three compounds with the B3LYP method adding polarization and diffuse basis sets at the B3LYP/6-31+G* level of approximation. The conformational properties are very similar to the previously described. Although the predicted relative energies $\Delta E°$ (corrected by zero-point energy) between the main conformers are lower than that computed at the B3LYP/6-31G level the trend is similar and both calculations favor the conformer similar to that found in the X-ray molecular structure by at least 8 kcal mol$^{-1}$. For each molecule here studied, the most stable conformer has been further optimized by using the more extended triple-zeta 6-311+G* basis sets. Selected geometrical parameters are given in Table 1. In general, this method predicts geometrical parameters for the molecular skeleton with values similar to those obtained from the X-ray analysis. Main differences are associated with the orientation of both the fluorinated and chlorinated phenyl rings with respect to the central carbonyl-thiourea moiety. Thus, computed dihedral angles around the C2–C1 bond are systematically higher than the experimental ones, by ca. 27°. On the other hand, while a nearly planar arrangement for the F-phenyl group is computed, dihedral angle of 45.8(4)°, 50.3(5)° and 40.0(5)° are determined from the X-ray molecular structure for compounds **1**–**3**, respectively.

### 2.3. Vibrational analysis

Experimental and calculated (B3LYP/6-311+G*) frequencies and intensities are given in Table 2. A tentative assignment of the observed bands was carried out by comparison with spectra of related molecules [20–28]. Very recently, the vibrational properties of the thiourea molecule – the idealized parent species – were revisited by Srinivasan et al. [29].

Quantum chemical calculations for compounds **1**–**3** isolated in a vacuum compute that the $\nu$(N1−H) stretching mode appears shifted to higher frequencies as compared with the $\nu$(N2−H) fundamental, whereas the integrated intensity is much higher for the later. The experimental infrared spectra present intense and very broad IR absorptions centered at 3158 cm$^{-1}$, which are assigned to the N−H stretching modes. These values agree with the corresponding ones in the IR spectrum of substituted thiourea [30] and thiocarbamate [27,31] compounds where $\nu$(N–H) is typically observed in the 3200 cm$^{-1}$ region. The broad features observed in the infrared spectra suggest that in solids **1**–**3** the amidic and ureasic protons do take part in intramolecular and/or intermolecular hydrogen bonding, in agreement with the results found in the crystal structure determination.

The strong IR absorptions at 1684, 1682 and 1682 cm$^{-1}$ for compounds **1**–**3**, respectively, were assigned to the $\nu$(C=O) modes. Very strong counterparts are observed in the Raman spectra at 1685, 1682 and 1682 cm$^{-1}$ for the studied compounds. Calculated (B3LYP/6-311++G**) frequencies for this mode are also very similar for the three isomers (1724, 1720 and 1719 cm$^{-1}$), indicating that the F-substituted phenyl rings have a little influence on the amide group. It is worthy to mention that the C=O stretching mode is appreciably coupled with the C–N stretch and with the N–H bend, as observed for related compounds [32,33].

In relation to the spectroscopic peculiarities of substituted phenyl groups, characteristic group wave numbers are observed. One of them is the 1595 cm$^{-1}$ (**1** and **2**) and 1591 cm$^{-1}$ (**3**) absorptions that mainly originates in an antisymmetric stretching mode of the benzene ring. As reported for the related species [33], these modes are calculated to be also strongly coupled with other vibrational modes.

It is well-known that both the amide and thiourea groups present a characteristic band in the 1500–1600 cm$^{-1}$ range of the IR spectrum, originated by the N−H deformation mode [$\delta$(N−H)]. For the title species, very strong IR absorptions with defined maxima at 1536 cm$^{-1}$ (**1** and **2**) and 1542 cm$^{-1}$ (**3**), are assigned to these modes. Strong signals are also observed in the Raman spectra at 1540, 1539 and 1544 cm$^{-1}$, respectively. Taking compound **1** as illustration, B3YLP/6-311+G* computations predict a strong band due to the $\delta$(N2−H) normal mode at 1607 cm$^{-1}$, whereas the $\delta$(N1−H) is predicted at lower wave numbers (1569 cm$^{-1}$).

A well-defined strong absorption can be observed in the 1400–1300 cm$^{-1}$ region in the infrared spectra of the studied

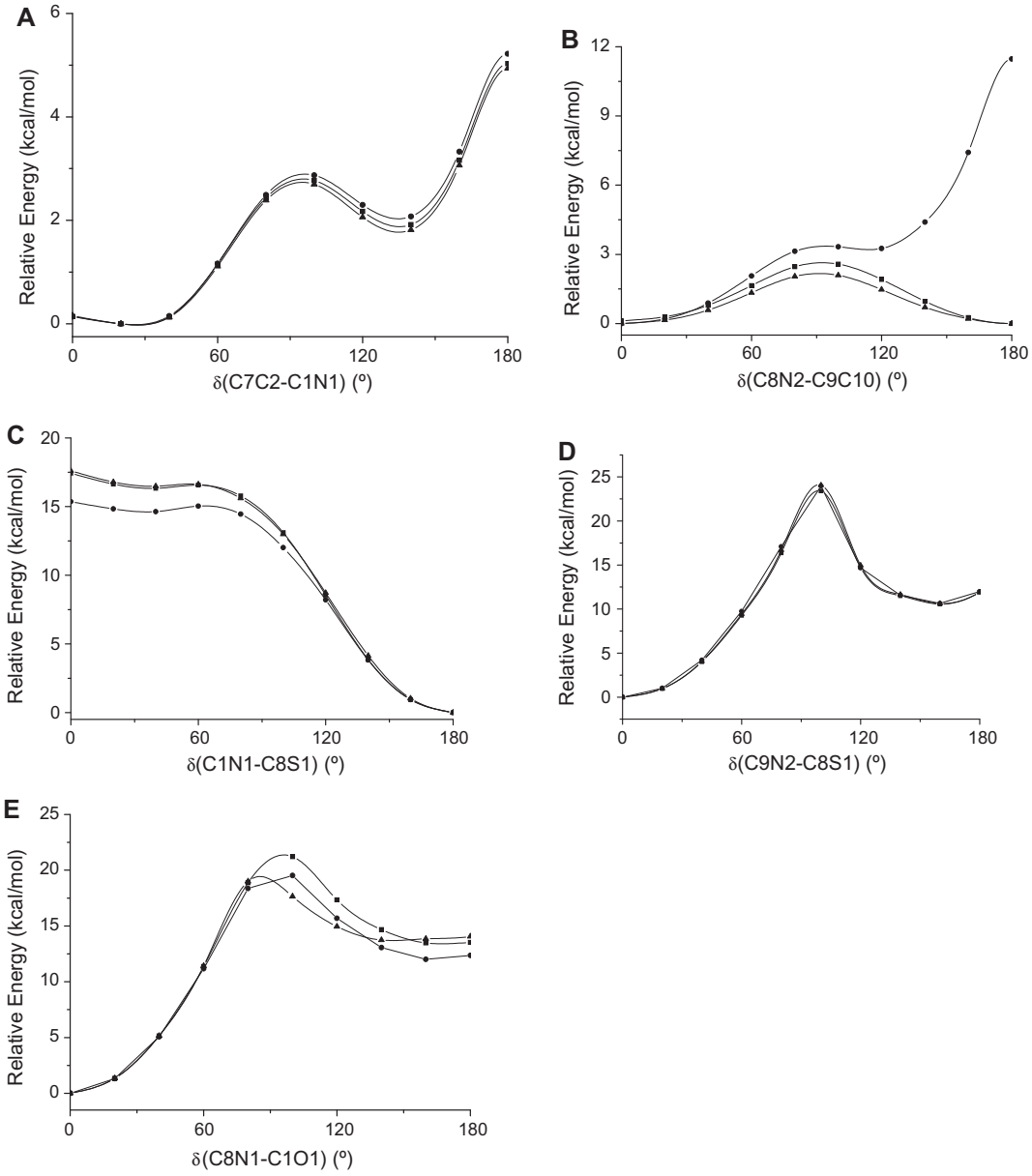


**Fig. 7.** Calculated (B3LYP/6-31G) potential function for internal rotation of compounds **1** (●), **2** (▲) and **3** (■) as a function of the $\delta$(C7C2−C1N1) (A), $\delta$(C8N2−C9C10) (B), $\delta$(C1N1−C8S1) (C), $\delta$(C9N2−C8S1) (D) and $\delta$(C8N1−C1O1) (E) dihedral angles. For atom numbering see Figs. 1–3.

compounds. Taking into account the vibrational properties reported for the simple thiourea molecule [29], it is expected that the C–N stretching modes, which are usually coupled in symmetric and antisymmetric motions, appear in this region [32]. The situation becomes more complicated if, as for compounds **1**–**3**, there are inequivalent C–N bonds. Thus, the NCN antisymmetric stretching mode of the thiourea moiety is assigned to the intense bands centered at 1335, 1335 and 1345 $cm^{-1}$ in the infrared spectra of compounds **1**–**3**, respectively. Computed values at the B3LYP/6-311+G* level of approximation are 1385, 1386 and 1394 $cm^{-1}$, respectively, slightly higher than the experimentally observed ones. The symmetric counterparts, with lower intensity, appear at ca. 1280 $cm^{-1}$ in the IR spectra of compounds **1**–**3** (computed values are 1277, 1284 and 1275 $cm^{-1}$, respectively). These modes are better defined in the Raman spectra, where strong signals appear at 1281, 1280 and 1285 $cm^{-1}$. The C–N stretching related with the N1–C1 in the amide group appears in the same region and were tentatively assigned to the absorptions observed at 1261 (1257, Raman), 1275 (1267, Raman) and 1258 (1256, Raman) $cm^{-1}$ in the IR spectrum of the title compounds, respectively, in assignments with reported data for related species [24,28,30].

The IR absorptions observed at 1099, 1078 and 1099 $cm^{-1}$ were assigned to the $\nu$(C=S) mode for compounds **1**–**3**, in good agreement with the calculated values (Table 2). In the thiourea molecule, this mode appeared in the 1094 $cm^{-1}$ in the infrared spectrum (1105 $cm^{-1}$ Raman) [30], while higher values – up to 1325 $cm^{-1}$ – have been also reported [25]. The formation of C=S···H–X intermolecular hydrogen bonds seems to strongly affect the frequency of the $\nu$(C=S) mode [20]. The values for the $\nu$(C=S) stretching mode observed in the IR spectra of the title compounds can be associated with the formation of intermolecular hydrogen bonds involving the thiocarbonyl group, as determined in the X-ray analysis.

Finally, the $\nu$(C–F) stretching mode is quite insensitive to the position of the fluorine atom, and originates medium intensity infrared absorptions at 1239, 1245 and 1236 $cm^{-1}$, for the studied isomers, with the corresponding signals appearing at 1240, 1242 and 1234 $cm^{-1}$ in the Raman spectra, respectively. Similarly,

**Table 2**
Observed and theoretical vibrational data ($cm^{-1}$) for isomers **1**–**3**.

| FTIR[a] | | | FT-Raman[a] | | | Calculated[b] | | | Proposed assignment/ approximate description |
|---|---|---|---|---|---|---|---|---|---|
| **1** | **2** | **3** | **1** | **2** | **3** | **1** | **2** | **3** | |
| 3232 sh | 3225 sh | 3225 sh | | | | 3605 (42.4) | 3604 (42.3) | 3605 (41.8) | ν(N1–H) |
| 3158 vsbr | 3158 vsbr | 3157 vsbr | | | | 3372 (288.3) | 3389 (285.0) | 3390 (273.1) | ν(N2–H) |
| | | | | | | 3251 (7.1) | 3256 (6.8) | 3249 (8.1) | ν(C–H, F-Ph) |
| | | | 3077 m | 3076 sh | 3087 m | 3209 (7.2) | 3208 (7.8) | 3209 (7.4) | ν(C–H, Cl-Ph) |
| | | | | | 3072 sh | 3205 (2.9) | 3206 (5.2) | 3205 (3.0) | ν(C–H, Cl-Ph) |
| 3058 m | 3058 m | 3060 m | 3060 m | 3062 s | 3060 s | 3204 (8.3) | 3204 (3.4) | 3204 (4.4) | ν(C–H, F-Ph) |
| | | | | | | 3192 (10.4) | 3192 (9.7) | 3199 (5.5) | ν(C–H, Cl-Ph) |
| 3022 m | 3015 m | 3015 m | | | 3012 w | 3191 (19.3) | 3187 (0.1) | 3192 (10.5) | ν(C–H, F-Ph) |
| | | | | | | 31,785 (2.5) | 3182 (10.9) | 3178 (2.3) | ν(C–H, Cl-Ph) |
| | | | | | | 3177 (2.4) | 3178 (2.2) | 3169 (6.2) | ν(C–H, F-Ph) |
| 1684 vs | 1682 vs | 1682 vs | 1685 vs | 1682 vs | 1682 vs | 1724 (136.6) | 1721 (113.1) | 1719 (136.9) | ν(C=O) |
| 1616 w | | 1610 m | 1617 vs | 1613 m | 1607 s | 1648 (133.9) | 1669 (207.9) | 1665 (401.9) | ν(C–C, F-Ph) |
| | | | | | | 1635 (51.3) | 1635 (49.9) | 1653 (0.4) | ν(C–C, Cl-Ph) |
| 1595 m | 1595 m | 1591 m | 1589 | 1595 m | 1592 sh | 1623 (344.4) | 1652 (405.2) | 1635 (332.6) | ν(C–C, F-Ph) |
| 1556 vs | 1551 vs | 1555 vs | 1567 w | 1591 sh | 1568 w | 1607 (173.3) | 1609 (205.5) | 1620 (202.8) | δ(N2–H) |
| | | | | 1569 w | | 1606 (92.2) | 1606 (17.0) | 1606 (17.2) | ν(C–C, Cl-Ph) |
| 1536 vs | 1536 vs | 1542 vs | 1540 s | 1539 m | 1544 s | 1569 (399.7) | 1568 (454.8) | 1570 (464.7) | δ(N1–H) |
| 1492 vs | 1492 vs | 1507 vs | 1513 w | 1509 sh | 1511 m | 1524 (143.8) | 1529 (170.) | 1545 (310.5) | ν(C–C, F-Ph) |
| 1458 m | 1472 m | 1470 m | 1493 w | 1493 m | 1494 w | 1503 (14.1) | 1503 (14.9) | 1503 (15.2) | ν(C–C, Cl-Ph) |
| 1436 s | 1436 s | 1436 s | | | | 1494 (34.7) | 1471 (40.1) | 1469 (40.9) | ν(C–C, F-Ph) |
| | | 1414 | | 1437 w | 1413 w | 1468 (33.1) | 1466 (14.1) | 1450 (2.3) | ν(C–C, Cl-Ph) |
| 1335 s | 1335 s | 1345 s | | | | 1385 (646.8) | 1386 (695.1) | 1394 (563.4) | $\nu_{as}$(NCN) |
| | | | 1334 w | | 1339 | 1349 (57.2) | 1354 (58.7) | 1346 (34.7) | ν(C–C, F-Ph) |
| | | | 1304 m | | 1304 m | 1320 (3.7) | 1334 (16.4) | 1332 (7.2) | ν(C–C, Cl-Ph) |
| | | | 1291 s | 1291 sh | 1293 m | 1318 (3.4) | 1321 (3.5) | 1320 (5.9) | ν(C–C, F-Ph) |
| 1290 sh | 1293 sh | | | | | 1300 (54.9) | 1300 (56.6) | 1301 (84.1) | ν(C1–C2) |
| 1280 s | 1280 s | 1282 s | 1281 s | 1280 m | 1285 m | 1277 (35.3) | 1284 (72.6) | 1275 (128.3) | $\nu_s$(NCN) |
| 1261 m | 1275 m | 1258 m | 1257 s | 1267 w | 1256 s | 1251 (112.3) | 1258 (105.4) | 1246 (94.6) | ν(C1–N1) |
| 1239 m | 1245 m | 1236 s | 1240 s | 1242 m | 1234 s | 1216 (110.6) | 1201 (36.7) | 1238 (73.8) | ν(C–F) |
| 1209 m | | 1214 m | 1207 w | | | 1192 (82) | 1193 (1.9) | 1192 (1.6) | ν(C–C, Cl-Ph) |
| | 1187 w | 1169 w | 1171 sh | 1188 w | 1174 m | 1187 (38.4) | 1178 (151.0) | 1188 (38.9) | δ(C–H, F-Ph) |
| 1164 s | 1160 s | 1160 s | 1158 s | 1161 m | 1158 s | 1172 (171.3) | 1166 (111.1) | 1172 (236.1) | $\nu_s$(CN1C) |
| 1128 w | 1140 m | 1130 w | 1128 w | 1139 m | | 1148 (13.3) | 1149 (14.2) | 1149 (12.9) | δ(C–H, Cl-Ph) |
| 1108 w | 1106 w | 1106 w | | 1103 w | | 1122 (16.9) | 1106 (47.0) | 1135 (5.1) | δ(C–H, F-Ph) |
| 1099 m | 1078 m | 1099 m | 1099 m | 1078 w | 1099 m | 1102 (29.4) | 1100 (18.0) | 1101 (55.7) | ν(C=S) |
| 1047 w | 1047 w | 1047 w | 1036 sh | 1047 vw | | 1061 (7.5) | 1060 (16.5) | 1060 (17.9) | ν(C9–N2) |
| | 1028 w | 1032 w | 1030 vs | 1029 s | 1032 s | 1058 (15.9) | 1055 (34.4) | 1055 (33.1) | δ(CCC, Cl-Ph) |
| | 1006 w | 1014 m | | 1006 vs | | 1055 (34.7) | 1023 (4.4) | 1031 (5.0) | δ(CCC, Cl-Ph) |
| | | | | | | 999 (0.7) | 1008 (1.9) | 999 (0.7) | δ(C–H, Cl-Ph) |
| | 984 w | 986 vw | | 983 m | | 984 (0.4) | 1000 (0.7) | 970 (4.3) | δ(C–H, F-Ph) |
| 955 w | 949 w | 955 m | | | | 971 (3.8) | 980 (0.2) | 966 (9.9) | δ(N–C–N) |
| 940 m | | 940 m | 944 s | | 943 m | 967 (8.4) | 968 (1.0) | 965 (0.2) | δ(C–H, Cl-Ph) |
| | | | | | | 944 (3.8) | 910 (38.2) | 942 (0.3) | δ(C–H, F-Ph) |
| | 894 m | 873 w | 860 w | 897 w | 864 s | 882 (1.9) | 898 (0.2) | 882 (1.7) | δ(C–H, Cl-Ph) |
| | | | | | | 871 (9.1) | 882 (2.0) | 873 (8.9) | δ(NC=O) |
| 853 m | 861 m | 861 m | | 860 vw | | 869 (1.2) | 874 (70.5) | 852 (107.5) | δ(C–H, F-Ph) |
| | | 840 m | | | 842 w | 852 (58.7) | 829 (40.7) | 834 (13.6) | ρ(N2–H) |
| 811 m | 815 m | 811 m | 813 w | 814 vw | 810 s | 821 (22.7) | 824 (5.8) | 826 (32.2) | δ(CCC, F-Ph) |
| | 788 w | 790 w | | | 784 w | 791 (22.5) | 789 (9.7) | 806 (0.2) | δoop(C=O) |
| 767 sh | 767 sh | 768 sh | 785 vw | | | 763 (58.4) | 784 (71.8) | 787 (25.1) | δ(N2C=S) |
| 753 s | 753 s | 753 s | 763 m | 748 m | 752 m | 762 (45.7) | 756 (29.9) | 754 (38.9) | δ(C–N2–C) |
| | | | 753 m | | 742 m | 754 (25.1) | 752 (10.2) | 746 (12.5) | δ(N1C=S) |
| 722 m | 722 m | 728 m | 715 w | 711 w | 725 w | 735 (30.4) | 735 (30.0) | 736 (30.5) | ν(C–Cl) |
| | | | | 699 sh, w | | 732 (0.3) | 703 (8.1) | 714 (0.1) | ρ(C–H, F-Ph) |
| | | | | | | 702 (7.7) | 688 (15.0) | 703 (6.9) | δ(CCC, F-Ph) |
| 708 w | | 707 w | | | 705 vw | 672 (10.4) | 677 (7.0) | 668 (13.9) | δ(CCC, Cl-Ph) |
| 690 w | 685 w | 693 w | 692 w | | 694 w | 660 (50.7) | 661 (55.9) | 659 (50.4) | ρ(N1–H) |
| 656 w | 659 w | 656 m | 654 w | 660 m | 654 m | 645 (4.8) | 650 (5.6) | 648 (6.5) | δ(CCC, Cl-Ph) |
| 632 w | 638 w | 634 w | 631 w | 640 w | 633 w | 607 (10.7) | 608 (0.1) | 620 (3.0) | δoopC=S |
| 621 m | 625 m | 624 m | | | 620 w | 576 (5.2) | 602 (11.6) | 600 (11.1) | δ(CCC, F-Ph) |
| 572 w | 569 w | 609 | 617 w | 620 w | | 563 (0.2) | 566 (7.5) | 548 (11.1) | δ(CCC, F-Ph) |
| 554 m | | 551 w | 555 vw | 559 w | | 538 (8) | 527 (5.3) | 525 (21.4) | δ(CCC, F-Ph) |
| 525 m | 524 m | 515 s | 524 vw | 519w | | 512 (7.2) | 492 (15.6) | 487 (17.8) | δ(CCC, Cl-Ph) |
| 469 w | 480 w | 468 w | 469 m | 460 m | 469 w | 481 (7.8) | 468 (4.4) | 450 (10.5) | δ(C–Cl) |
| 455 m | 460 m | 450 m | | | 447 w | 463 (5.8) | 464 (4.0) | 435 (13.9) | δ(CCC, F-Ph) |
| 445 vw | 451 vw | | 444 m | 447 w | 436 w | 444 (6.6) | 446 (4.0) | 425 (0.1) | δ(CCC, Cl-Ph) |
| 419 m | 419 m | | | 413 w | 416 w | 425 (4.9) | 425 (5.3) | 420 (0.5) | ρ(CCC, Cl-Ph) |
| | | 410 vw | 401 vw | | 382 w | 404 (18.6) | 415 (10.7) | 412 (15.7) | δ(C1C2C3) |
| | | 362 m | | 360 m | 361 m | 373 (5.7) | 375 (5.4) | 373 (10.3) | ρ(C=O) |
| | | 323 m | | 327 w | 316 vw | 315 (0.6) | 313 (3.8) | 338 (0.1) | δ(C10C9N2) |
| | | 285 w | | | 302 vw | 310 (2.6) | 273 (0.7) | 310 (1.6) | ρ(C–F) |
| | | 256 m | | 258 m | 259 m | 262 (4.4) | 266 (2.7) | 281 (1.2) | ρ(CCC, Cl-Ph) |

**Table 2** (*continued*)

| FTIR[a] | | | FT-Raman[a] | | | Calculated[b] | | | Proposed assignment/ approximate description |
|---|---|---|---|---|---|---|---|---|---|
| **1** | **2** | **3** | **1** | **2** | **3** | **1** | **2** | **3** | |
| | | 223 w | | 235 m | 220 w | 228 (0.6) | 238 (0.1) | 243 (3.4) | $\rho$(CCC, F-Ph) |
| | | | | | | 227 (1.1) | 232 (1.5) | 228 (1.2) | $\rho$(C=S) |
| | | 205 w | | 203 w | 200w | 198 (4.2) | 206 (0.7) | 181 (0.2) | $\rho$(CCC, F-Ph) |
| | | 177 m | | 174 m, sh | 180 m | 185 (4) | 194 (9.0) | 179 (5.3) | $\rho$(CCC, Cl-Ph) |
| | | 158 sh | | | 157 sh | 155 (0.7) | 157 (0.4) | 153 (0.2) | $\rho$(C–Cl) |
| | | | | 131 s | 134 sh | 112 (2.8) | 111 (3.2) | 112 (3.3) | $\rho$(C1–C2) |
| | | | | | | 95 (3.2) | 95 (2.1) | 95 (3.0) | $\rho$(N2-Ph) |
| | | | | | | 82 (0.7) | 85 (1.5) | 73 (1.8) | $\tau$ |
| | | | | | | 58 (1.1) | 55 (0.5) | 54 (0.5) | $\tau$ |
| | | | | | | 31 (0.7) | 31 (0.5) | 28 (0.2) | $\tau$ |
| | | | | | | 17 (0.5) | 19 (1.0) | 16 (0.2) | $\tau$ |
| | | | | | | 10 (0.8) | 12 (0.5) | 12 (0.2) | $\tau$ |

[a] FTIR of solid in KBr pellets.
[b] B3LYP/6-311+G* level of approximation.

medium intensity bands at 722 $cm^{-1}$ (compounds **1** and **2**) and 728 $cm^{-1}$ (compound **3**) were assigned to the $\nu$(C–Cl) stretching modes.

## 3. Conclusions

Three novel 1-(2-chlorobenzoyl)-3-(isomeric fluorophenyl)-thiourea derivatives (**1**–**3**) were prepared by treating 2-chlorobenzoyl isothiocyanate produced *in situ* with isomeric fluoroanilines in excellent yields. Conformational and structural properties were determined by using experimental techniques which include infrared spectroscopy as well as X-ray diffraction analysis. Results derived from the quantum chemical calculations show that the central – C=O–NH–C=S–NH – moiety adopts a planar structure with a preferred antiperiplanar orientation of both C=O and C=S double bonds. This form is present in crystalline **1**–**3** compounds as centro-symmetric dimeric units mainly held by N–H···S=C hydrogen bonds. The conformational preference is conserved for the three studied isomers and fluorine substitution slightly affects the preferred orientation adopted by the fluoro-phenyl group with respect to the thiourea group.

## 4. Experimental

### 4.1. Synthesis and characterization

The 1-(2-chlorobenzoyl)-3-(substituted fluorophenyl)thiourea derivatives (**1**–**3**) were prepared by the reaction of 2-chlorobenzoyl isothiocyanate produced *in situ* with isomeric fluoroanilines in excellent yields (Scheme 1). The IR, $^{1}H$, $^{13}C$ NMR and GC–MS spectral data of thioureas (**1**–**3**) are given in Table 3. 2-Fluoroaniline, the 3-fluoroaniline and 4-fluoroaniline, potassium thiocyanate as well as 2-chlorobenzoyl, were purchased from Aldrich and used as received. 2-Chlorobenzoyl chloride was treated in a 1:1 M ratio with potassium thiocyanate in dry acetone to afford the 2-chlorobenzoyl isothiocyanate intermediate which was not separated. Condensation of the latter with isomeric fluoroanilines furnished the 1-(2-chlorobenzoyl)-3-(substituted fluorophenyl)thiourea derivatives (**1**–**3**) in 75–87% yields. The melting points were recorded using a digital Gallenkamp (SANYO) model MPD.BM 3.5 apparatus and are as follows: 164–165, 129–130 and 170–171 °C for (**1**–**3**), respectively. $^{1}H$ and $^{13}C$ NMR spectra were recorded in $CDCl_3$ at 300 MHz and 75 MHz respectively with a Bruker 300 MHz spectrophotometer and elemental analyses were conducted using a LECO-183 CHNS analyzer.

### 4.2. Vibrational spectroscopy

The reactions were monitored by measuring IR spectra of the solid products on an IR Shimadzu 460 spectrophotometer as KBr pellets. Moreover, after purification crystals were selected and solid-phase IR spectra were recorded with a resolution of 2 $cm^{-1}$ in the 4000–400 $cm^{-1}$ range on a Bruker EQUINOX 55 FTIR spectrometer.

### 4.3. GC–MS determination

The GC–MS measurements were recorded in a GCMS-QP2010 SHIMADZU instrument using gaseous Helium as mobile phase with

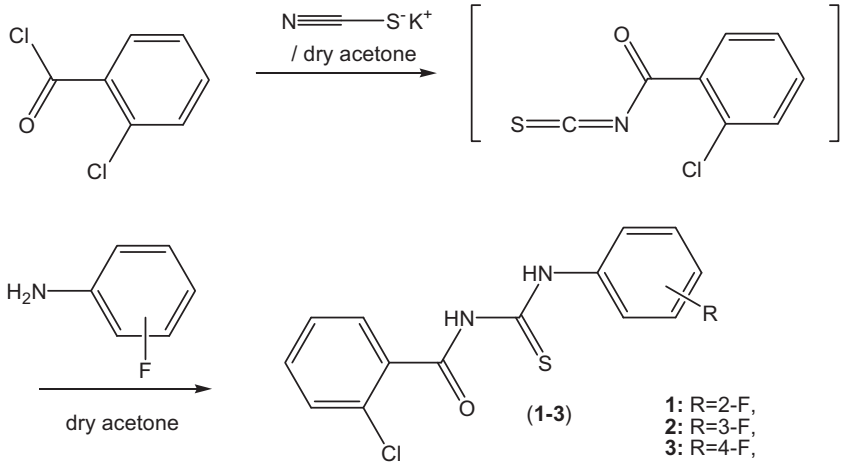


**Scheme 1.** Synthesis of 1-(2-chlorobenzoyl)-3-(isomeric fluorophenyl)thioureas.

**Table 3**
Infrared spectra, $^{1}H$, $^{13}C$ nuclear magnetic resonance spectra and mass spectrometry data for synthesized thioureas **1–3**.

| | IR | $^{1}H$ NMR | $^{13}C$ NMR | MS |
|---|---|---|---|---|
| 1 | 3225, 3158 broad, s (*ν*N–H), 1682 vs. (C=O), 1595 m (C=C), 1536 vs. (*δ*N–H), 1335 s (*ν*CN), 1078 m (*ν*C=S) | 12.48 (*br s*, 1H, NH), 9.34 (*br s*, 1H, NH), 8.44 (*dt*, *J* = 2.1, 7.5 Hz, 1H, Ar–H), 7.83 (*td*, *J* = 0.9, 7.2 Hz, 1H, Ar–H), 7.55–7.18 (*m*, 7H, Ar–H) | 177.9 (C=S), 165.9 (C=O), 155.1 (*d*, $^{1}J$ = 247 Hz), 133.5, 131.8, 131.2, 131.0, 130.8, 127.8 (*d*, $^{3}J$ = 8.25 Hz), 127.6, 125.3, 124.1 (*d*, $^{4}J$ = 3.75 Hz), 125.94 (*d*, $^{3}J$ = 10.5 Hz), 115.97 (*d*, $^{2}J$ = 19.5 Hz) | 197(1%, $ClC_6H_4CONCS^+$), 139(100%, $ClC_6H_4CO^+$), 111(47%, $ClC_6H_4^+$), 75(33%, $NHCSNH_2$?), 32(8%, $S^+$) |
| 2 | 3232, 3158 broad, s (*ν*N–H), 1684 (*ν*C=O), 1595 (*ν*C=C), 1536 vs. (*δ*N–H), 1335 s (*ν*CN), 1099 m (*ν*C=S) | 12.49 (*br s*, 1H, NH), 9.33 (*br s*, 1H, NH), 7.79–6.97 (*m*, 8H, Ar–H) | 177.6 (C=S), 166.2 (C=O), 165.6 (*d*, $^{1}J$ = 245 Hz), 138.9 (*d*, $^{3}J$ = 10.5 Hz), 133.5, 131.9, 131.2, 131.0, 130.5, 130.6 (*d*, $^{3}J$ = 9.75 Hz), 127.6, 119.4 (*d*, $^{4}J$ = 3 Hz), 113.7 (*d*, $^{2}J$ = 21.75 Hz), 111.2 (*d*, $^{2}J$ = 26.25 Hz) | 197(1%, $ClC_6H_4CONCS^+$), 139(100%, $ClC_6H_4CO^+$), 111(46%, $ClC_6H_4^+$), 75(33%, $NHCSNH_2$?), 32(7%, $S^+$) |
| 3 | 3225, 3157 broad, s (*ν*N–H), 1682 vs. (C=O), 1591 m (C=C), 1542 vs. (*δ*N–H), 1345 s (*ν*CN), 1099 m (*ν*C=S) | 12.29 (*br s*, 1H, NH), 9.34 (*br s*, 1H, NH), 7.77 (*dd*, *J* = 1.2, 8.1 Hz, 1H, Ar–H), 7.70–7.10 (*m*, 7H, Ar–H) | 178.3 (C=S), 166.2 (C=O), 161.0 (*d*, $^{1}J$ = 246 Hz), 133.5, 133.4, 132.0, 131.2, 131.0, 130.5, 127.6, 126.3 (2C, *d*, $^{3}J$ = 8.25 Hz), 115.8 (2C, *d*, $^{2}J$ = 22.5 Hz) | 197(1%, $ClC_6H_4CONCS^+$), 139(100%, $ClC_6H_4CO^+$), 111(48%, $ClC_6H_4^+$), 75(35%, $NHCSNH_2$?), 32(7%, $S^+$) |

the pressure in the column head equal to 100 kPa. The column used was a 19091J-433 HP-5 of 30 m × 0.32 mm × 0.25 mm film thickness. A 1 μL volume of the compounds dissolved in $CHCl_3$ was chromatographed under the following conditions: injector temperature was 210 °C, the initial column temperature (100 °C) was held for 3 min, then increased to 200 °C at 20 °C/min and held for 2 min after elevated to 300 °C at 35 °C/min and held for 2 min. In the spectrometer the source was kept at 200 °C. One peak at retention time 8.4 min is observed in the chromatogram, with a similar fragmentation pattern for three isomers (see Table 3).

### 4.4. Quantum chemical calculations

All quantum chemical calculations were performed with the GAUSSIAN 03 program package [34]. The molecular geometries were optimized to standard convergence criteria by using a DFT hybrid method with Becke's non-local three parameter exchange and the Lee, Young and Parr correction (B3LYP) using 6-31+G* and the more extended 6-311+G* basis sets. The calculated vibrational properties corresponded in all cases to potential energy minima for which no imaginary frequency was found.

**Table 4**
Crystal data and structure refinement for compounds **1–3**[a].

| Compound | 1 | 2 | 3 |
|---|---|---|---|
| Formula weight | 308.75 | 308.75 | 308.75 |
| Crystal system | Monoclinic | Monoclinic | Monoclinic |
| Space group | C2/c | C2/c | C2/c |
| *a*/Å | 20.319(3) | 20.3792 | 20.4725 |
| *b*/Å | 7.2553(11) | 7.3148(8) | 7.4141(18) |
| *c*/Å | 18.790(3) | 18.954(2) | 18.297(4) |
| *β*° | 97.922(3) | 98.0193 | 99.6874 |
| *V*/Å3 | 2743.6(7) | 2797.9(5) | 2737.5(11) |
| *Z* | 8 | 8 | 8 |
| Dc/Mgm$^{-3}$ | 1.495 | 1.466 | 1.498 |
| Absorp. coeff./mm$^{-1}$ | 0.438 | 0.429 | 0.438 |
| *F*(0 0 0) | 1264 | 1264 | 1264 |
| Crystal size/mm$^3$ | 0.51 × 0.49 × 0.45 | 0.39 × 0.30 × 0.25 | 0.51 × 0.50 × 0.47 |
| *Data collection* | | | |
| *h* | −26/26 | −26/26 | −26/26 |
| *k* | −9/9 | −9/9 | −9/9 |
| *l* | −22/24 | −24/24 | −24/24 |
| Data collected | 11,392 | 11,908 | 11,267 |
| Unique reflections | 3277 | 3341 | 3260 |
| *R*(int) | 0.0183 | 0.0264 | 0.0242 |
| Max/min transm. | 0.827/0.807 | 0.900/0.850 | 0.820/0.807 |
| Parameters | 188 | 188 | 188 |
| GooF | 1.038 | 1.049 | 1.078 |
| *R*1[*I* > 2sigma(*I*)] | 0.0283 | 0.03791 | 0.0339 |
| w*R*2 (all data) | 0.0772 | 0.0964 | 0.0929 |
| Max/min *δF*/e Å$^{-3}$ | 0.344/−0.195 | 0.392/−0.232 | 0.447/−0.329 |
| CCDC deposition numbers | 742,706 | 742,705 | 742,707 |

[a] Further conditions and refinement comments: temperature, 120(2) K, wavelength 0.71073 Å, Theta ranges/° = 2.02–27.88, absorption correction: semi-empirical from equivalents, refinement method: full-matrix least-squares on $F^2$.

### 4.5. X-ray data collection, structure solution and refinement

Crystals of the thioureas were grown by slow evaporation of 1:1 by volume acetone–anhydrous ethanol mixtures at room temperature. Pertinent crystal and refinement data for **1–3** are given in Table 4. Bruker-AXS SMART APEX CCD [35] graphite monochromator, *λ*(Mo Kα) = 0.71073 Å. Structures solved by direct methods, full-matrix least-squares refinement based on $F^2$. All but H-atoms refined anisotropically. Hydrogen atoms were located from difference Fourier maps and refined at idealized positions riding on the carbon atoms with isotropic displacement parameters $U_{iso}(H) = 1.2U_{eq}(C)$. H(N) atom parameters were refined freely.

## Acknowledgments

MFE is member of the Carrera del Investigador of CONICET (República Argentina). The Argentinean authors thank to the Consejo Nacional de Investigaciones Científicas y Técnicas (CONICET), the ANPCYT and to the Facultad de Ciencias Exactas, Universidad Nacional de La Plata for financial support.

## References

[1] D.A. Burrows, D.C. Mare, F.M. Mahon, Polyhedron 18 (1999) 2665–2671.
[2] W. Henderson, B.K. Nicholson, M.B. Dinger, R.L. Bennett, Inorg. Chim. Acta 338 (2002) 210–218.
[3] K.R. Koch, Coord. Chem. Rev. (2001) 473–488.
[4] M. Krunks, J. Madarasz, L. Hiltunen, R. Mannonen, E. Mellikov, L. Niinisto, Acta Chem. Scand. 51 (1997) 294–301.
[5] X. Du, E. Hansell, J.C. Engel, C.R. Caffrey, F.E. Cohen, J.H. McKerrow, Chem. Biol. 7 (2000) 733–742.
[6] C. Sun, H. Huang, M. Feng, X. Shi, X. Zhang, P. Zhoub, Bioorg. Med. Chem. Lett. 16 (2006) 162–166.
[7] R. Krishnamurthy, S. Govindaraghavan, J. Narayanasamy, Pestic. Sci. 52 (1999) 145–151.
[8] L. Nie, Z. Li, J. Han, X. Zhang, R. Yang, W.-X. Liu, F.-Y. Wu, J.-W. Xie, Y.-F. Zhao, Y.-B. Jiang, J. Org. Chem. 69 (2004) 6449–6454.
[9] P. Zlatušková, I. Stibor, M. Tkadlecová, P. Lhoták, Tetrahedron 60 (2004) 11383–11390.
[10] H. Park, J. Choi, S. Choi, M. Park, J. Lee, Y. Suh, H. Cho, U. Oh, J. Lee, S.-U. Kang, J. Lee, H.-D. Kim, Y.-H. Park, Y.S. Jeong, J.K. Choi, S. Jew, Bioorg. Med. Chem. Lett. 14 (2004) 787–791.
[11] X. Sijia, D. Liping, K. Shaoyong, J. Liangbin, Chem. J. Internet 5 (2003) 67–70.
[12] T.P. Yoon, E.N. Jacobsen, Angew. Chem. Int. Ed. 44 (2005) 466–468.
[13] T. Okino, S. Nakamura, T. Furukawa, Y. Takemoto, Org. Lett. 6 (2004) 625–627.
[14] H.B. Huang, E.N. Jacobsen, J. Am. Chem. Soc. 128 (2006) 7170–7171.
[15] M. Boiocchi, L. Del Boca, D.E. Gomez, L. Fabbrizzi, M. Licchelli, E. Monzani, J. Am. Chem. Soc. 126 (2004) 16507–16514.

[16] W.-X. Liu, R. Yang, A.-F. Li, Z. Li, Y.-F. Gao, X.-X. Luo, Y.-B. Ruan, Y.-B. Jiang, Org. Biomolec. Chem. 7 (2009) 4021–4028.
[17] D. Makuc, M.A. Triyanti, J. Plavec, K. Rissanen, A. Valkonen, C.A. Schalley, Eur. J. Org. Chem. 28 (2009) 4854–4866.
[18] G.N. Lipunova, E.V. Nosova, A.A. Laeva, T.V. Trashakhova, P.A. Slepukhin, V.N. Charushin, Russ. J. Org. Chem. 44 (2008) 741–749.
[19] L. Farrugia, J. Appl. Cryst. 30 (1997) 565.
[20] P.P. Tadbuppa, E.R.T. Tiekink, Acta Cryst. E63 (2007) o1779–o1780.
[21] J. Dillen, M.G. Woldu, K.R. Koch, Acta Cryst. E62 (2006) o4819–o4820.
[22] J. Dillen, M.G. Woldu, K.R. Koch, Acta Cryst. E62 (2006) o5228–o5229.
[23] J. Dillen, M.G. Woldu, K.R. Koch, Acta Cryst. E62 (2006) o5225–o5227.
[24] J. Goerdeler, A. Schulze, Chem. Ber. 115 (1982) 1252–1255.
[25] C.G. Overberger, H.A. Friedman, J. Polym. Sci. A3 (1965) 3625–3634.
[26] S. Torrico-Vallejos, M.F. Erben, H. Willner, R. Boese, C.O. Della Védova, J. Org. Chem. 72 (2007) 9074–9080.
[27] H. Arslan, U. Flörke, N. Kulcu, Spectrochim. Acta 67A (2007) 936–943.
[28] S. Torrico-Vallejos, M.F. Erben, R. Boese, O.E. Piro, E.E. Castellano, C.O. Della Védova, J. Mol. Struct. 918 (2009) 146–153.
[29] K. Srinivasan, S. Gunasekaran, S. Krishnan, Spectrochim. Acta 75A (2010) 1171–1175.
[30] B. Rousseau, C. Van Alsenoy, R. Keuleers, H.O. Desseyn, J. Phys. Chem. A 102 (1998) 6540–6548.
[31] S. Torrico-Vallejos, M.F. Erben, O.E. Piro, E.E. Castellano, C.O. Della Védova, Polyhedron 28 (2009) 937–946.
[32] W. Kolodziejski, I. Wawer, K. Wozniak, J. Klinowski, J. Phys. Chem. A 97 (1993) 12147–12152.
[33] V. Arjunan, S. Mohan, S. Subramanian, B. Thimme Gowda, Spectrochim. Acta 60A (2004) 1141–1159.
[34] M.J.T. Frisch, G.W. Schlegel, H.B. Scuseria, G.E. Robb, M.A. Cheeseman, J.R. Montgomery Jr., J.A. Vreven, T. Kudin, K.N. Burant, J.C. Millam, J.M. Iyengar, S.S. Tomasi, J. Barone, V. Mennucci, B. Cossi, M. Scalmani, G. Rega, N. Petersson, G.A. Nakatsuji, H. Hada, M. Ehara, M. Toyota, K. Fukuda, R. Hasegawa, J. Ishida, M. Nakajima, T. Honda, Y. Kitao, O. Nakai, H. Klene, M. Li, X. Knox, J.E. Hratchian, H.P. Cross, J.B. Adamo, C. Jaramillo, J. Gomperts, R. Stratmann, R.E. Yazyev, O. Austin, A.J. Cammi, R. Pomelli, C. Ochterski, J.W. Ayala, P.Y. Morokuma, K. Voth, G.A. Salvador, P. Dannenberg, J.J. Zakrzewski, V.G. Dapprich, S. Daniels, A.D. Strain, M.C. Farkas, O. Malick, D.K. Rabuck, A.D. Raghavachari, K. Foresman, J.B. Ortiz, J.V. Cui, Q. Baboul, A.G. Clifford, S. Cioslowski, J. Stefanov, B.B. Liu, G. Liashenko, A. Piskorz, P. Komaromi, I. Martin, R.L. Fox, D.J. Keith, T. Al-Laham, M.A. Peng, C.Y. Nanayakkara, A. Challacombe, M. Gill, P.M.W. Johnson, B. Chen, M.W. Wong, C. Gonzalez, J.A. Pople, Gaussian 03; Revision B.04 ed., Gaussian, Inc., Pittsburgh PA, 2003.
[35] G. Sheldrick, Acta Cryst. A64 (2008) 112–122;
Bruker, SMART (Ver. 5.62), SAINT (Ver. 6.02), SHELXTL (Ver. 6.10), Bruker AXS Inc., Madison, Wisconsin, USA, 2002.